Effect of rotational diffusion on quasielastic light scattering from fractal colloid aggregates

H. M. Lindsay
Corporate Research Science Laboratories, Exxon Research and Engineering Company, Route 22 East, Annandale, New Jersey 08801

R. Klein
Fakultät für Physik, Universität Konstanz, Postfach 55 60, D-7750 Konstanz, West Germany

D. A. Weitz
Corporate Research Science Laboratories, Exxon Research and Engineering Company, Route 22 East, Annandale, New Jersey 08801

M. Y. Lin
Corporate Research Science Laboratories, Exxon Research and Engineering Company, Route 22 East, Annandale, New Jersey 08801 and Department of Physics, City College of the City University of New York, New York, New York 10031

P. Meakin
Corporate Research and Development Department, E.I. du Pont de Nemours and Company, Experimental Station, Wilmington, Delaware 19189

(Received 22 March 1988)

We examine the contribution of rotational diffusion to quasielastic light scattering (QELS) from fractal colloid aggregates, both theoretically and experimentally. Rotational diffusion makes a substantial contribution to QELS when the size of the clusters is large compared with the inverse of the scattering wave vector, due to the anisotropy of the clusters at all length scales smaller than the cluster size. We evaluate the rotational contributions to QELS by performing a multipole expansion of the light scattered from computer-simulated clusters. Experimentally, rotational contributions are observed through measurement of the wave-vector dependence of the first cumulant. We find excellent agreement between cumulants calculated through our multipole-expansion technique and those obtained in our experimental measurements.

INTRODUCTION

Considerable progress has been made in recent years in our understanding of kinetic colloid aggregation.[1–6] A key to this progress is the recognition of the scale invariant structure of the aggregates, allowing them to be well characterized as fractals. This in turn has allowed more detailed study of colloidal aggregation by a variety of techniques, among which light scattering has been quite prominent. To date, the almost universally used parameter for characterizing the structure of the aggregates is their fractal dimension d_f. While d_f is clearly an extremely important parameter, it cannot, by itself, fully describe the highly disordered structure that typifies an aggregate. In particular, the fractal dimension reflects a radially averaged quantity, and provides no information about structural features that are not rotationally symmetric. However, many physical properties of colloidal aggregates are sensitive to their anisotropy, making a structural characterization beyond the fractal dimension essential. An example of one such physical property is quasielastic light scattering (QELS), which has been widely and successfully used in studies of the dynamics of colloid aggregation. QELS is a measure of the intensity fluctuations of the scattered light caused by the motion of the clusters. Because of the structural anisotropy of a fractal object, the light intensity scattered by an aggregate changes as it rotates. Thus both rotational and translational diffusion must be included to fully exploit QELS in studies of colloid aggregation.[6] In this paper, we develop the theoretical formalism necessary to account for the contribution of rotational diffusion to QELS, and demonstrate its importance by comparing our calculations to experimental measurements.

We present a description of the structure of colloidal aggregates that goes beyond the fractal dimension to characterize the anisotropy of the clusters. This is achieved by performing a multipole expansion of their structure using computer-simulated clusters. By doing this in momentum space we can directly determine the contribution of rotational diffusion to the temporal autocorrelation function of the scattered light intensity. We calculate the full intensity autocorrelation function as is measured experimentally, to correctly determine the relative mixing of the contributions of rotational and translational motion to the fluctuations. In addition, we explicitly test the validity of the Siegert relationship[7] to fractal aggregates, to determine when the intensity autocorrelation function can be represented by the square of the field autocorrelation function. Our results are compared to the experimental measurements using very well characterized colloidal gold aggregates. We show that rotation-

al diffusion plays a crucial role in understanding the QELS data as the cluster size increases so that $kR_g > 1$, where k is the scattering wave vector and R_g the radius of gyration of the cluster. Indeed, the resultant k dependence of the QELS data can provide an experimental measure of the structural anisotropy of the aggregate. Excellent agreement is obtained between our measurements and calculations.

The calculation of the multipole terms shows that the fractal clusters not only possess structure on all length scales, but also possess anisotropy on all length scales. It is this feature which leads to the importance of the contribution of rotational diffusion in QELS. The behavior of the multipole terms provides a more complete description of both the structure and the anisotropy of highly disordered fractal clusters, allowing a more detailed comparison of aggregates formed in different ways. In addition, the scaling behavior of the multipole terms may provide an alternate technique for defining a hierarchy of fractal dimensions based solely on structure rather than the more usual method based on growth probabilities.[8]

LIGHT SCATTERING FROM FRACTAL AGGREGATES

We motivate the need for considering the rotational anisotropy of fractal aggregates by Fig. 1, which shows a transmission electron micrograph of a cluster composed of gold particles of 75-Å radius. This cluster is typical of those created under diffusion-limited conditions,[9] and has a fractal dimension of ~ 1.8. The fractal dimension for these aggregates has been determined through several means; by measuring cluster mass versus radius, yielding the relation $M \propto R^{d_f}$; by measuring the two-particle correlation function for the component particles in the cluster, $g(r) \propto r^{d_f - 3}$; and by measuring the static structure factor of the clusters $S(k) \propto k^{-d_f}$ with light,[6] x-ray,[10] and neutron scattering.[3] These methods lead to consistent values for the fractal dimension of these clusters.. By changing the aggregation conditions to reaction limited, a second class of fractal clusters is produced, with $d_f \sim 2.1$.[11]

The techniques used to find the fractal dimension all measure radially averaged quantities. However, as is apparent in Fig. 1, the fractal clusters are isotropic only in a statistically averaged sense. Their shape is in fact highly anisotropic, and this anisotropy extends to all length scales, and therefore will have a profound impact upon light scattering, since the scattered intensity depends on the orientation of the cluster when the scattering vector is large enough to be sensitive to the internal structure. Thus an understanding of the effects of this anisotropy is of key importance in interpreting light scattering data.

We illustrate the consequences of the anisotropy in Fig. 2, where we show the calculated intensity of light scattered by a single cluster as a function of its orientation about an arbitrary axis. We use an aggregate consisting of 900 particles which is generated by computer simulation of diffusion-limited cluster-cluster aggregation (DLCA). The scattering data in Fig. 2 are obtained through summation of the phase factors of the light scattered,

$$I(k,\theta) = \left| \sum_i e^{i\mathbf{k}\cdot\mathbf{r}_i} \right|^2 , \tag{1}$$

where $\mathbf{k}$ is the scattering wave vector and $\mathbf{r}_i$ is the position of the ith particle. The top curve shows the light scattered when $kR_g \ll 1$, so that the internal structure of the cluster is not resolved and the scattering intensity is independent of orientation. The middle curve shows the light scattered from the same cluster when $kR_g = 1$. Now the internal structure of the cluster is beginning to be resolved, resulting in an orientation dependence of the scattering. The lowest curve shows the light scattered from the cluster when $kR_g \gg 1$. Here the internal structure of the cluster is well resolved, leading to very large variations of the scattered intensity with orientation. Therefore, when $kR_g \gtrsim 1$, as is often the case experimen-

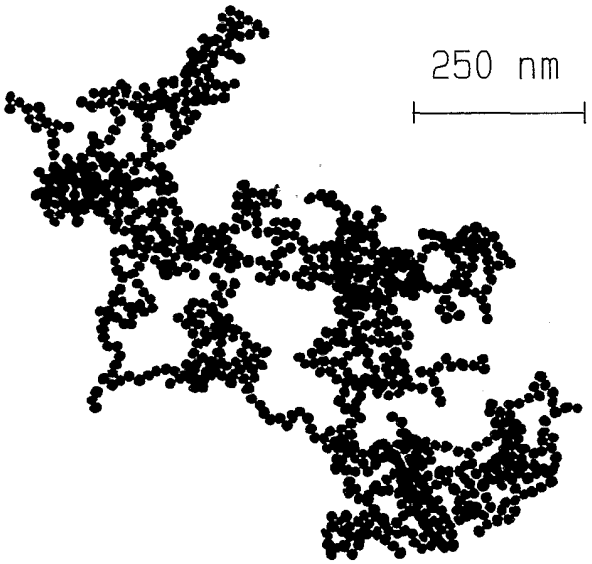

FIG. 1. Transmission electron micrograph of colloidal gold aggregate formed under diffusion-limited aggregation conditions.

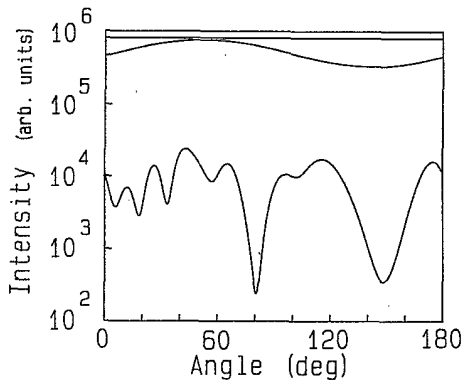

FIG. 2. Calculated intensity of scattered light from a simulated DLCA cluster made up of 900 particles, as a function of rotation about an arbitrary axis. In the top curve, $kR_g = 0.1$; in the middle curve, $kR_g = 1$; in the bottom curve, $kR_g = 10$.

tally, orientationally averaged quantities are insufficient to provide a complete description of light scattering from fractal colloidal aggregates. For example, choosing a different axis for the same cluster illuminated in Fig. 2 would result in a completely different curve.

Static light scattering experiments probe the structure factor, which reflects an orientational and ensemble average of the scattered intensity. Therefore the fluctuations evident in Fig. 2 are not observed and only radially averaged quantities are measured. Experimentally, the scattered light intensity is time averaged sufficiently long to average the fluctuations and obtain a true average. By contrast QELS is a direct measure of the magnitude and time dependence of the fluctuations in the scattered light intensity. In large part, these fluctuations result from the relative motion of different clusters due to their translational diffusion. However, as is clearly shown in Fig. 2, if $kR_g \gtrsim 1$, the anisotropy of the clusters also leads to fluctuations in the scattered intensity as they undergo rotational diffusion. The calculation of the magnitude and time dependence of these rotationally induced fluctuations cannot be accomplished using radially averaged quantities, but instead requires knowledge of the separate multipole terms that comprise the structure factor. Each of these terms has a different time dependence when the cluster undergoes rotational diffusion. Thus a determination of the multipole terms, and their time dependence, is essential to properly interpret the effects of rotational diffusion on QELS.

THEORY

In quasielastic light scattering we study the temporal fluctuations of the scattered light by measuring the temporal autocorrelation function of the intensity.[12] QELS experiments can be divided into two classes; homodyne and heterodyne. In a homodyne experiment, only the light scattered by the sample is observed; in a heterodyne experiment, the scattered light is mixed with a portion of the incident laser light which serves as a reference oscillator. The fluctuations in the scattered intensity probed in a QELS experiment can come from several sources. First, the particles in the sample may move, causing a change in the path length of the light scattered to the detector, and consequently a change in the phase of the electric field at the detector. In a heterodyne experiment, variations in the phase of the scattered field relative to the reference beam lead to fluctuations in the measured intensity; this method is sensitive to changes in the absolute position of the particles in the sample. In homodyne scattering, the variation in the phase of the scattered field due to the motion of the particles relative to the other particles in the sample cause the fluctuations in the scattered intensity; homodyne measurements are insensitive to the mean velocity of the scattering system, and detect only their relative translations. We note that a heterodyne experiment can in principle probe the translation of a single particle, whereas a homodyne experiment requires at least two particles to probe a relative displacement.

A second cause of scattering fluctuations is the rotation of the scatterers if they are anisotropic and when $kR_g \gtrsim 1$. A homodyne QELS experiment is sensitive to the rotational diffusion from a single cluster, whereas two clusters are required for a contribution from translational diffusion. Physically, when $kR_g > 1$, the scattering from a single fractal cluster can be considered to comprise of contributions from $(kR_g)^{d_f}$ independent clusters each of size $\sim k^{-3}$, and all rigidly connected. A rotation changes the relative position of these subclusters, resulting in a contribution to a homodyne QELS experiment.

In this paper we determine the contribution of rotational diffusion to QELS from fractal clusters. Our method is a generalization of the one used previously to calculate the effect of the rotation of a rigid rod on QELS.[13] We represent the autocorrelation function in terms of a multipole expansion and then calculate both the magnitude and decay rate as a function of the wave vector for each term using computer-simulated clusters. Normally it is sufficient to calculate the field autocorrelation function and to square it to obtain the intensity autocorrelation function, using the Siegert relationship.[7] However, as we illustrated in Fig. 2, the scattered intensity from a single cluster fluctuates as it rotates, and this contribution would not be included within the field autocorrelation function calculated by the standard approximation. In order to ascertain the importance of this contribution, as well as to determine the correct mixing of the contributions of rotational and translational motions, we calculate the full intensity autocorrelation function $I_2(k,t)$. We expand the intensity autocorrelation function[14,15] and determine the contributions from each term, allowing us to test the range of validity of the Siegert relationship for fractal aggregates where the coherence length is the size of the cluster itself, and is typically considerably larger than k^{-1}. At later states of aggregation, there may be relatively few independent coherence volumes within the detection volume, requiring the verification of the validity of the Siegert relationship.

We begin by denoting the scattered electric field from an ensemble of N clusters, $\alpha=1,2,\ldots,N$. If n_α represents the number of particles in the αth cluster, then

$$E_s(k,t)=E_0\sum_{\alpha=1}^{N}\sum_{j=1}^{n_\alpha}P_j^\alpha e^{i\mathbf{k}\cdot\mathbf{r}_j^\alpha(t)}, \tag{2}$$

where $\mathbf{r}_j^\alpha(t)$ is the position of the jth particle in the αth cluster at time t, $\mathbf{k}$ is the scattering wave vector, E_0 is the magnitude of the incident electric field, and P_j^α is the polarizability of each particle. We set $E_0=1$ with the assumption that the field scattered from each particle is proportional to the incident field times a phase factor.[16] This is an excellent approximation for fractal aggregates, even for the case of gold, as shown by Chen,[17] although the polarizability must be renormalized to reflect local field corrections. We assume that each cluster is comprised of identical spheres. In this work we examine only the I_{VV} polarized light scattering, with scattering wave vectors smaller than the inverse of a particle diameter; therefore we ignore the form factor of the individual spheres and set $P_j=1$. We assume that the concentration of aggregates is sufficiently low that they are noninteracting, so that the motions and positions of different clusters are uncorrelated. We also assume that our scattering volume is sufficiently large that the clusters remain in the

scattering volume over experimental time scales, allowing us to ignore number fluctuation contributions to QELS;[18] this condition is generally met experimentally. Thus, we have for the intensity autocorrelation function,

$$I_2(k,t)=\langle\,|E_s(k,t)|^2\,|E_s(k,0)|^2\rangle = \sum_{\alpha,\beta,\gamma,\delta}\sum_{j,k,l,m}\langle\exp(i\mathbf{k}\cdot[-\mathbf{r}_j^{\alpha}(t)+\mathbf{r}_k^{\beta}(t)-\mathbf{r}_l^{\gamma}(0)+\mathbf{r}_m^{\delta}(0)]\}\rangle\ . \tag{3}$$

Decomposing the position of the ith particle in the αth cluster in terms of the position of the center of mass of the cluster, $\mathbf{R}_\alpha(t)$, and the displacement of the particle from that center of mass, $\mathbf{b}_i^{\alpha}(t)$,

$$\mathbf{r}_i^{\alpha}(t)=\mathbf{R}_\alpha(t)+\mathbf{b}_i^{\alpha}(t)\ , \tag{4}$$

we then write the autocorrelation function as

$$I_2(k,t)=\sum_{\alpha,\beta,\gamma,\delta}\sum_{i,j,k,l}\langle\exp\{i\mathbf{k}\cdot[-\mathbf{R}_\alpha(t)+\mathbf{R}_\beta(t)-\mathbf{R}_\gamma(0)+\mathbf{R}_\delta(0)]\}\exp\{i\mathbf{k}\cdot[-\mathbf{b}_i^{\alpha}(t)+\mathbf{b}_j^{\beta}(t)-\mathbf{b}_k^{\gamma}(0)+\mathbf{b}_l^{\delta}(0)]\}\rangle\ . \tag{5}$$

Since different clusters are uncorrelated, the contributions of most combinations of the indices will vanish. There are three distinct conditions to obtain a nonzero contribution. The first condition is $\alpha=\beta$, $i=j$, $\gamma=\delta$, $k=l$, $\alpha\neq\gamma$, which just gives the average scattering intensity, which is the time-independent background of the autocorrelation function

$$I_2^B=\sum_{\substack{\alpha,\gamma\\(\alpha\neq\gamma)}}\sum_{i=1}^{n_\alpha}\sum_{k=1}^{n_\gamma}\langle 1\rangle=\sum_{\substack{\alpha,\gamma\\(\alpha\neq\gamma)}} n_\alpha n_\gamma\ . \tag{6}$$

This background term can be ignored in the rest of our calculations; in analyzing an experimental measurement of an intensity autocorrelation function, the background value is subtracted from the data before further analysis is done.

For time-dependent contributions to the autocorrelation function, we require in Eq. (5) that $\alpha=\gamma$ and $\beta=\delta$. This correlates the scattered fields from each cluster at time t with the scattered fields from the same cluster at time 0. We can further distinguish two possibilities. When $\alpha=\beta$, only terms involving single clusters are examined. Thus the first exponential in Eq. (5), which reflects translational diffusion, does not contribute, as expected, since a homodyne experiment is insensitive to the absolute position of a cluster. By contrast, the orientation of a single cluster does cause fluctuations in the scattered intensity, so only rotational diffusion can contribute to this set of terms. In the other case, when $\alpha\neq\beta$, two distinct clusters are involved; both the relative positions of two clusters and their orientation cause fluctuations in the scattered light intensity, so both translational and rotational diffusion contribute. This yields

$$I_2(k,t)=I_2^{(1)}(k,t)+I_2^{(2)}(k,t)+I_2^B\ , \tag{7}$$

where

$$I_2^{(1)}(k,t)=\sum_{\alpha}\sum_{i,j,k,l}\langle\exp\{i\mathbf{k}\cdot[-\mathbf{b}_i^{\alpha}(t)+\mathbf{b}_j^{\alpha}(t)-\mathbf{b}_k^{\alpha}(0)+\mathbf{b}_l^{\alpha}(0)]\}\rangle \tag{8}$$

and

$$I_2^{(2)}(k,t)=\sum_{\alpha,\ \beta(\neq\alpha)}\sum_{i,j,k,l}\langle\exp\{i\mathbf{k}\cdot[\mathbf{R}_\alpha(t)-\mathbf{R}_\alpha(0)]\}\exp\{i\mathbf{k}\cdot[\mathbf{R}_\beta(t)-\mathbf{R}_\beta(0)]\}\times\exp\{i\mathbf{k}\cdot[\mathbf{b}_i^{\alpha}(t)-\mathbf{b}_j^{\alpha}(0)]\}\exp\{i\mathbf{k}\cdot[\mathbf{b}_k^{\beta}(t)-\mathbf{b}_l^{\beta}(0)]\}\ . \tag{9}$$

We now see that the autocorrelation function consists of two components, $I_2^{(1)}(k,t)$, which depends only on the orientation of the clusters (and hence on rotational diffusion), and $I_2^{(2)}(k,t)$, which depends both on position and orientation. From the summations involved, we note that $I_2^{(1)}$ will scale with the number of clusters in the scattering volume N, while $I_2^{(2)}$ scales with N^2. In most experimental situations, N is sufficiently large that $I_2^{(1)}$ may be ignored; nevertheless, we shall retain the $I_2^{(1)}$ term in order to explicitly evaluate its effects.

For simplicity, we assume that translational and rotational diffusion of a cluster are uncoupled, and that each cluster is characterized by a single translational diffusion coefficient determined by the Stokes relation, $D_\alpha=k_BT/6\pi\eta R_H^{\alpha}$. Here k_B is Boltzmann's constant, T the temperature, η the viscosity of the solvent, and R_H^{α} is the hydrodynamic radius of the αth cluster. The assumptions of a single translational diffusion coefficient and uncoupled rotational and translational motion are reasonable so long as the overall anisotropy of the clusters is not too large. We then express the terms involving the center of mass coordinates of the clusters in terms of the translational diffusion coefficients. We can also separate the orientational terms for different clusters, since the clusters are uncorrelated, and write $I_2^{(2)}$ as

$$I_2^{(2)}(k,t)=\sum_{\alpha,\ \beta(\neq\alpha)}e^{-k^2D_\alpha t}e^{-k^2D_\beta t}\sum_{i,j,k,l}\langle\exp\{i\mathbf{k}\cdot[\mathbf{b}_i^{\alpha}(t)-\mathbf{b}_j^{\alpha}(0)]\}\rangle\langle\exp\{i\mathbf{k}\cdot[\mathbf{b}_k^{\beta}(t)-\mathbf{b}_l^{\beta}(0)]\}\rangle = \sum_{\alpha,\ \beta(\neq\alpha)}e^{-k^2D_\alpha t}e^{-k^2D_\beta t}I_R^{\alpha}(t)I_R^{\beta}(t)\ . \tag{10}$$

To perform the averages in $I_2^{(2)}$ we use the Rayleigh expansion

$$e^{i\mathbf{k}\cdot\mathbf{b}_i(t)}=4\pi\sum_{l,m} i^l j_l(kb_i)Y^*_{lm}(\Omega_k)Y_{lm}[\Omega_i(t)]\ , \tag{11}$$

where j_l is the lth spherical Bessel function, Y_{lm} denotes spherical harmonics, Ω_k is the orientation of the scattering vector, and $\Omega_i(t)$ is the orientation of the displacement vector $\mathbf{b}_i(t)$ in the laboratory frame. Thus

$$I_R^\alpha(t)=\sum_{i,j}4\pi\Big\langle\sum_{l,m}\sum_{l',m'} i^l(-i)^{l'}j_l(kb_i^\alpha)j_{l'}(kb_j^\alpha) \times Y^*_{lm}(\Omega_k)Y_{l'm'}(\Omega_k)Y_{lm}(\Omega_i^\alpha(t)) \times Y^*_{l'm'}(\Omega_j^\alpha(0))\Big\rangle\ . \tag{12}$$

We then assign to each cluster an arbitrary reference frame fixed to the cluster which rotates with the cluster in the laboratory frame. The cluster-fixed and laboratory frames are connected by the transformation Euler angles $\Omega_T=(\alpha,\beta,\gamma)$, and the spherical harmonics in the two frames are connected by the relation

$$Y_{lm}(\Omega_{\rm lab})=\sum_{m'} D^l_{m'm}(\Omega_T)Y_{lm'}(\Omega_{\rm cl})\ , \tag{13}$$

where the $D^l_{m'm}$ are the Wigner rotation matrices. Thus

$$I_R^\alpha(t)=\sum_{i,j}\Big\langle\sum_{l,m}\sum_{l',m'} i^l(-i)^{l'}j_l(kb_i^\alpha)j_{l'}(kb_j^\alpha)Y^*_{lm}(\Omega_k)Y_{l'm'}(\Omega_k)\sum_{M,M'}Y_{lM}(\Omega_i^\alpha)Y_{l'M'}(\Omega_j^\alpha)D^l_{Mm}(\Omega_T(t))D^{l'}_{M'm'}(\Omega_T(0))\Big\rangle\ , \tag{14}$$

where Ω_i^α now refers to the orientation of the ith particle in the reference frame fixed to the αth cluster. All of the time dependence is now in the transformation angles between the laboratory and cluster frames.

The time averaging which must be performed in the above expression may be expressed as[16]

$$\langle(\cdots)\rangle=\int d\Omega(0)\int d\Omega(t)(\cdots)G(\Omega(t),t\mid\Omega(0),0)\ , \tag{15}$$

where $G(\Omega(t),t\mid\Omega(0),0)$ is the joint probability distribution for the cluster-fixed coordinate system to have angles $\Omega(t)$ at time t and $\Omega(0)$ at time $t=0$. This probability distribution is a solution of the rotational diffusion equation for an arbitrary anisotropic diffusor. We simplify this quantity considerably by assuming that the clusters behaves like a sphere with hydrodynamic radius R_H^α, and has a single rotational diffusion coefficient $\Theta_\alpha=k_BT/6\pi\eta(R_H^\alpha)^3$. This simplification is based on our earlier assumption that the overall outlines of our clusters are not too anisotropic. Therefore[16]

$$G(\Omega_T(t),t\mid\Omega_T(0),0) =\frac{1}{8\pi^2}\sum_{J,K,M''}\frac{2J+1}{8\pi^2}D^J_{KM''}(\Omega_T(0))D^J_{KM''}(\Omega_T(t)) \times e^{-l(l+1)\Theta t} \tag{16}$$

and we obtain

$$\begin{aligned}\langle D^l_{Mm}(\Omega_T(t))D^{l'*}_{M'm'}(\Omega_T(0))\rangle &=\frac{1}{8\pi^2}\sum_{J,K,M''}\frac{2J+1}{8\pi^2}e^{-l(l+1)\Theta t}\int d\Omega_T(0)\int d\Omega_T(t)D^J_{KM''}(\Omega_T(0))D^{l'*}_{M'm'}(\Omega_T(0))D^l_{Mm}(\Omega_T(t))D^{J*}_{KM''}(\Omega_T(t))\\ &=\frac{1}{2l+1}\delta_{ll'}\delta_{MM'}\delta_{mm'}e^{-l(l+1)\Theta t}\ .\end{aligned} \tag{17}$$

Using Eqs. (14)–(17) above, and the relation

$$\sum_m|Y_{lm}(\Omega_k)|^2=\frac{2l+1}{4\pi}\ , \tag{18}$$

we find

$$\begin{aligned}I_R^\alpha(t)&=4\pi\sum_l\Big[\sum_{i,j}j_l(kb_i^\alpha)j_l(kb_j^\alpha) \times\sum_m Y_{lm}(\Omega_i^\alpha)Y^*_{lm}(\Omega_j^\alpha)\Big]e^{-l(l+1)\Theta_\alpha t}\\ &=4\pi\sum_{l,m}\Big|\sum_i j_l(kb_i^\alpha)Y_{lm}(\Omega_i^\alpha)\Big|^2e^{-l(l+1)\Theta_\alpha t}\ .\end{aligned} \tag{19}$$

Here we define a set of multipole expansion terms

$$S_l^\alpha(k)=\sum_m\Big|\sum_i j_l(kb_i^\alpha)Y_{lm}(\Omega_i^\alpha)\Big|^2\ . \tag{20}$$

Using Eqs. (19) and (20) in Eq. (10), we obtain

$$I_2^{(2)}(k,t)=\sum_{\alpha,\,\beta\,(\neq\alpha)}\sum_{l,l'}S_l^\alpha(k)S_{l'}^\beta(k)e^{-k^2(D_\alpha+D_\beta)t} \times e^{-[l(l+1)\Theta_\alpha+l'(l'+1)\Theta_\beta]t}\ . \tag{21}$$

Following a similar procedure

$$I_2^{(1)}(k,t)=\sum_\alpha\sum_{l,l'}S_l^\alpha(k)S_{l'}^\alpha(k)e^{-[l(l+1)+l'(l'+1)]\Theta_\alpha t}\ . \tag{22}$$

In examining the three contributions to the intensity autocorrelation functions, we find one term $I_2^B(k,t)$ which supplies a time-independent background and which scales as $N(N-1)$, where N is the number of clusters in the scattering volume; a second term, $I_2^{(2)}(k,t)$, which includes the product of rotational and translational contributions to the decay of the autocorrelation function, and also scales as $N(N-1)$; and finally a third term, $I_2^{(1)}(k,t)$, which depends solely on rotation, and scales as N. This last term confirms our intuition that a single cluster will be observed in a homodyne QELS experiment because its rotational diffusion results in a contribution to the intensity autocorrelation function, even though its translational motion does not contribute. However, its relative contribution will be unimportant in most experimental situations, when $N \gg 1$.

Finally, we compare the intensity autocorrelation function we have calculated with the field autocorrelation function $I_1(k,t)$ to test the validity of the Siegert relationship,[7]

$$I_2(k,t)=I_1^2(k,t)+B \ , \tag{23}$$

where B is a baseline. Writing the field autocorrelation function as

$$I_1(k,t)=\sum_\alpha e^{-D_\alpha k^2 t}\sum_l S_l^\alpha(k)e^{-l(l+1)\Theta_\alpha t} \ , \tag{24}$$

squaring this and comparing with Eq. (7), we see that

$$\begin{aligned} I_2(k,t)-I_2^B &= I_1^2(k,t)-\sum_\alpha\sum_{l,l'} S_l^\alpha(k)S_{l'}^\alpha(k)e^{-2D_\alpha^2 kt} \\ &\quad\times e^{-[l(l+1)+l'(l'+1)]\Theta_\alpha t} \\ &\quad + I_2^{(1)}(k,t) \ . \end{aligned} \tag{25}$$

The corrections to the Siegert approximation both scale as the number of clusters in the scattering volume N, while the autocorrelation function scales as N^2. Thus the Siegert approximation will be valid provided there are sufficient clusters in the scattering volume. Later in this paper we will numerically examine how large N needs to be.

CALCULATIONS

The key to evaluating the autocorrelation function is the evaluation of the multipole expansion terms $S_l^\alpha(k)$. It is these terms which provide the explicit contribution of the structural anisotropy to the light scattering. These terms can also provide a more detailed characterization of the fractal structure, including the anisotropy.[19] We have therefore examined numerically the behavior of these multipole expansion terms. We note that we chose to evaluate the terms in momentum space to directly determine the consequences for light scattering. Their real space behavior has also been studied very recently for a different type of fractal aggregate.[20]

In order to calculate the $S_l^\alpha(k)$ multipole terms for a cluster, it is necessary to know the positions of each particle within the cluster. We therefore use clusters generated by computer simulations of the experimental conditions, for both diffusion-limited cluster-cluster aggregation and reaction-limited cluster-cluster aggregation.[4,21] In our calculations we set the single particle radius to 75 Å to correspond with that of the gold colloid studied experimentally. The computer simulations use rules that correspond well to experimental regimes, and result in clusters that have the same fractal dimension as measured experimentally. Furthermore, the cluster mass distributions of the simulations are in agreement with those measured experimentally.[22] This gives us confidence that the simulated clusters provide good models of the experimentally produced clusters.

In Fig. 3, the $l=0$–7 multipole terms are shown for an ensemble of 20 DLCA clusters, each containing 900 particles. The large fluctuations present in the results for a single cluster are reduced by an ensemble average over many clusters of the same mass. When $kR_g \ll 1$, the $l=0$ multipole term dominates the scattering, implying that only translational diffusion contributes to QELS. This result is expected, since at long length scales the internal structure of the cluster is not resolved so it looks like a point scatterer. The $l=0$ term is constant at small k, and then declines at larger wave vectors. For $l>1$, the multipole terms rise at small wave vectors as k^{2l}, reach a peak value when $kR_g \sim l$, and then decline at higher k. The wave-vector dependence of the multipole terms is all contained in the spherical Bessel functions in Eq. (20). When $kR_g \ll 1$, all of the Bessel functions in the multipole terms are in their small argument limit, and scale as k^l. The $l>0$ terms contribute appreciably to the scattering only when they are at wave vectors greater than or equal to their peak. The sum of the first 7 multipole terms is also shown in Fig. 3. This sum is just the static structure factor, which by definition is averaged over all orientations of the clusters. This can be seen explicitly by comparing the static structure factor with the sum of the multipole expansion terms for a single cluster, The static structure factor can be evaluated using Eq. (1) and averaging the results over orientations. As shown in Fig. 4, the results are virtually identical.

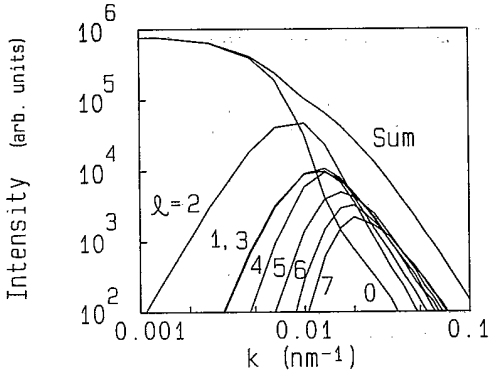

FIG. 3. Multipole expansion terms averaged over 20 DLCA clusters made up of 900 particles each vs scattering wave vector k. The multipole terms for $l=0$ to 7 are shown; the uppermost curve is the sum of the first seven multipole terms shown.

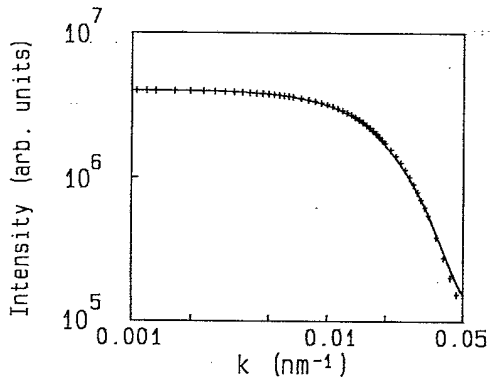

FIG. 4. Static structure factor for a 900 particle cluster, as calculated from the sum of the $l=0$ to 12 multipole terms (solid line), and through explicit calculation of the scattering from the cluster, averaged over 100 orientations (crosses).

In evaluating the intensity autocorrelation function, it is necessary to consider not only the amplitude of the multipole terms but also their rotational and translational decay rates. For a cluster of hydrodynamic radius R_H^α, the relevant time scale for translational diffusion is proportional to R_H^α/k^2 while for rotational diffusion the time scales as $(R_H^\alpha)^3/[l(l+1)]$, independent of the scattering vector. It is apparent that for small scattering vectors, rotational diffusion will be much faster than translational diffusion. However, the amplitude of the higher-order $S_l^\alpha(k)$ terms is so small that the $l=0$ term dominates, so the decay of the autocorrelation function is due solely to translation. At larger wave vectors, the higher-order terms become dominant in magnitude, while the decay rates for translation and rotation become comparable.

The consequences of the rotational diffusion on the autocorrelation function become apparent upon examination of the magnitudes of the multipole terms shown in Fig. 3 and their contribution to the decay shown in Eq. (21). When $kR_g > 1$, the autocorrelation function is a sum of exponentials, rather than a single exponential. Thus rotational diffusion affects the autocorrelation function in a fashion analogous to polydispersity in the size of scatterers. For a monodisperse set of noninteracting Brownian spheres, the QELS autocorrelation function measured is just a single exponential. If there is a distribution of spheres with different sizes the autocorrelation function is the sum of exponentials with different amplitudes and decay rates. Thus any comparison of the calculations to experimental data must include a determination of the contribution of both effects, polydispersity as well as rotational diffusion. This is particularly important if the QELS data are to be used to determine a true hydrodynamic radius which characterizes the distribution when $kR_g > 1$.

Rather than consider the entire autocorrelation function, we define the first cumulant Γ_1

$$\Gamma_1 = -\lim_{t\to 0}\left[\frac{d}{dt}\ln\left[\frac{I(k,t)}{I(k,0)}\right]\right] . \tag{26}$$

This defines the effective hydrodynamic radius $R = k^2 k_B T/6\pi\eta\Gamma_1$, which includes the contribution of rotational diffusion. We cannot therefore directly calculate the true hydrodynamic radius from Γ_1; however, we can calculate the first cumulant of the measured autocorrelation function for any distribution of clusters, and use this cumulant to characterize the sample. Using our earlier results,

$$\Gamma_1(k) = \left[\sum_{\alpha,\,\beta\,(\neq\alpha)}\sum_{l,l'} S_l^\alpha(k)S_{l'}^\beta(k)[k^2(D_\alpha+D_\beta)+l(l+1)\Theta_\alpha+l'(l'+1)\Theta_\beta] + \sum_\alpha\sum_{l,l'} S_l^\alpha(k)S_{l'}^\alpha(k)[l(l+1)\Theta_\alpha+l'(l'+1)\Theta_\alpha]\right]\left[\sum_{\alpha,\,\beta\,(\neq\alpha)}\sum_{l,l'} S_l^\alpha(k)S_{l'}^\beta(k)+\sum_\alpha\sum_{l,l'} S_l^\alpha(k)S_{l'}^\alpha(k)\right]^{-1} . \tag{27}$$

In examining the wave-vector dependence of the first cumulant, we divide by k^2 to remove the trivial dependence. The remaining k dependence is due to a combination of rotational diffusion and polydispersity. If the polydispersity can be minimized, the dependence of Γ_1/k^2 on k can be used to directly measure the consequences of the high-order multipole terms and therefore rotational diffusion.

In order to calculate Γ_1, we must know three terms for each cluster: $S_l^\alpha(k)$, D_α, and Θ_α. The multipole terms are evaluated numerically, using the positions of the component particles of each cluster. To obtain D_α and Θ_α we need to determine the hydrodynamic radius R_H^α of the cluster, since $D_\alpha = k_B T/6\pi\eta R_H^\alpha$ and $\Theta_\alpha = k_B T/8\pi\eta(R_H^\alpha)^3$. For our simulated clusters we calculate the radius of gyration R_g^α, and then use the scaling relation between R_H^α and R_g^α for fractal clusters, $R_H^\alpha = \beta R_g^\alpha$ (Ref. 23). The proportionality constant β is important, since the smaller β is, the larger is the effect of rotations. This proportionality constant depends on d_f and has been calculated[23,24] and measured[25] for different classes of aggregation clusters. In this paper we consider only diffusion-limited clusters and use $\beta = 0.87$.

Finally, we note that in our formalism we have characterized the clusters by a single hydrodynamic radius. This assumption should be valid if the overall asymmetry of the clusters is not too large. This should be contrasted with the anisotropy probed by our multipole expansion, which reflects the cluster structure at large kR_g, at length scales equal to or less than the cluster size. Measurement of the overall asymmetry of the simulated clusters indicates that the aspect ratio is less than 2, suggesting that

our approximation is reasonable.

An additional consideration in analyzing QELS data from colloidal aggregate samples is the number of clusters N available in the scattering volume. Since the total number of clusters decreases as the colloid aggregates, this number can potentially become very small in which case the Siegert relationship will not be valid. Earlier we discussed contributions to the autocorrelation function which scaled as the number of clusters N, while the generally dominant terms in the autocorrelation function scale as $N(N-1)$. We now examine how large N must be for these contributions to be negligible. We first compare $I_2^{(1)}$ with I_2. The most extreme case is when $N=1$. Since the intensity of light scattered by a single cluster does not depend on its position, translational diffusion will not give a contribution to the intensity autocorrelation function; however, rotational diffusion can give a contribution, due to the $I_2^{(1)}$ term.

For $N>1$, both translation and rotation contribute. In Fig. 5 we show Γ_1/k^2 versus k calculated for samples made of 1, 2, 10, and 100 identical clusters. We use identical clusters to eliminate any polydispersity effects, since even clusters with the same mass and radius would have different rotational contributions to the decay. For a single cluster, only rotational diffusion contributes, leading to the divergence seen at small k. However, even for $N=2$, at small k we recover the limit of pure translational diffusion as expected. We see that by $N=10$, we are almost at the large-N limit, where the decay is due to a product of both translational and rotational decays. Thus for pure rotational contributions to be significant, it is necessary to have only a very few clusters in the scattering volume; for dramatic effects, there must be only one.

We can also examine the validity of the Siegert approximation as a function of N. We do this by examining a polydisperse ensemble of clusters, using both the full calculation and Siegert approximation. We start with a pair of clusters of 100 and 1000 particles, and then reproduce this pair in order to achieve the large-N limit. The Siegert approximation remains unchanged as identical pairs of particles are added, while the full calculation in the intensity autocorrelation function approaches this limit. In Fig. 6 we plot Γ_1/k^2 versus k for the Siegert approximation and from $I_2(k,t)$. For $N=2$ the Siegert approximation is very poor; by $N=4$ the approximation is becoming reasonable. At $N=10$ only small corrections are needed, while at $N=100$ the Siegert approximation is nearly exact. Here we have chosen a severe case of polydispersity, providing the most challenge to the Siegert approximation; in a less polydisperse system, the small-N corrections would be less significant.

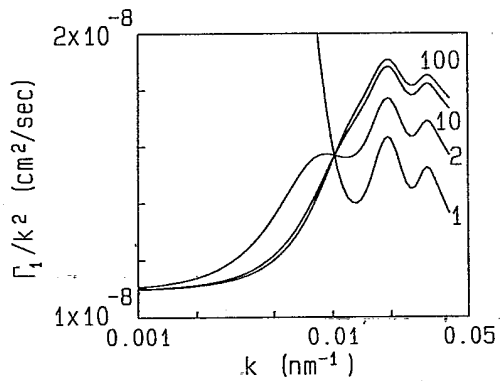

FIG. 5. Γ_1/k^2 vs k for 1, 2, 10, and 100 identical clusters. We assume that $\eta=0.96$ cP, suitable for water at 22 °C, and that the single particle radius is 75 Å.

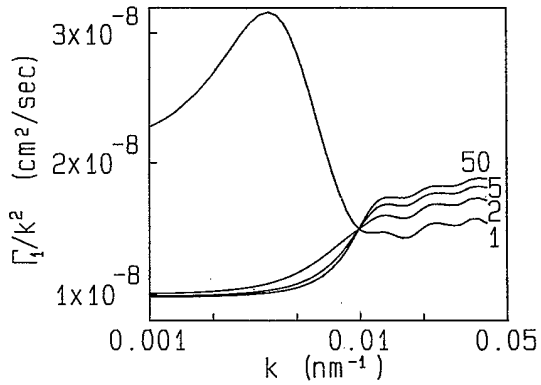

FIG. 6. Γ_1/k^2 vs k for 1, 2, 5, and 50 pairs of DLCA clusters made up of 100 and 1000 particles. The curve for the Gaussian approximation is indistinguishable from the 50 pair curve on this plot.

From the preceding argument, we see that if the number of clusters in the scattering volume is large, the calculation of the field autocorrelation function in Eq. (24), combined with the Siegert approximation, will be sufficient to describe QELS data. Therefore the cumulant for an ensemble of clusters will be the weighted average of the cumulants of the individual clusters. This provides a potential means of obtaining the true hydrodynamic radius from the measured Γ_1 even when rotations are important. For this, we first investigate the scaling of the first cumulant with cluster size. The wave-vector dependence of Γ_1/k^2 for a set of clusters with the same mass is shown in Fig. 5. When $kR_g \ll 1$, $\Gamma_1/k^2=D_0$, the Stokes diffusion coefficient; therefore, in comparing cluster of different masses, we scale the cumulant by D_0 for that cluster. In addition, we scale the k vector by the radius of gyration of the cluster. In Fig. 7 we plot $(\Gamma_1/k^2)/D_0$ as a function of kR_g for DLCA clusters of 100,200,300, . . . , 1000 particles. We see that the scaled cumulants all fall upon a single curve, indicating the scale invariance of the anisotropy of the DLCA clusters. The value of Γ_1/k^2 in Fig. 7 rises to a plateau value of ~ 1.7. The existence of this limiting value of Γ_1/k^2 at large wave vectors is expected from scaling arguments.[26] Further analysis of the scaling of the multipole expansion terms and their consequences will be discussed in a later work.[19]

The scaling with cluster size of the multipole expansion terms and the cumulants derived from them makes the calculation of the scattering from an ensemble of clusters much simpler, and is an absolute necessity when $kR_g \gtrsim 12$, where 12 is the order of the highest-order multipole term we can calculate numerically. In addition,

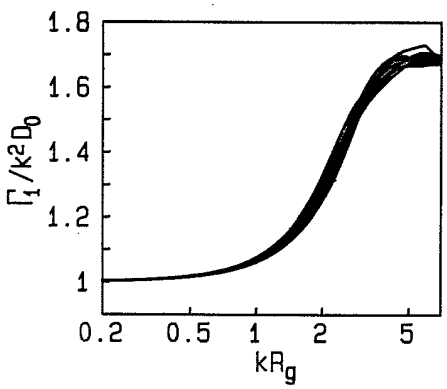

FIG. 7. Scaling of the first cumulants, showing $(\Gamma_1/k^2)/D_0$ vs kR_g for DLCA clusters of 100,200,300. . . ,1000 particles, using $\beta=0.87$.

this graph has a very important practical consequence. It can be used to correct for the effects of rotational diffusion, and thus determine the value of the hydrodynamic radius from the measured first cumulant, even when $kR_g > 1$. This condition is often unavoidable in the study of colloidal clusters, making this correction of great value.

EXPERIMENT

To experimentally test our calculations, we study the aggregation of colloidal gold, which has been extensively characterized using a variety of techniques. We begin with a sample of nearly monodisperse gold spheres of 75-Å radius suspended in water. The gold spheres have citrate ions on their surface, which provide the electrostatic repulsion necessary to prevent aggregation.[27] We can control the charge on the colloidal particles through the addition of pyridine; the neutral pyridine molecules displace the charged citrate ions from the surface of the gold. Before the addition of pyridine the repulsive barrier between the gold sphere is many times k_BT, and the colloid cannot aggregate. Through suitable addition of pyridine, we can lower the repulsive barrier to only a few k_BT; under these conditions, when two spheres come close together due to their diffusive motion, they are usually repelled, and do not stick, but occassionally can overcome the repulsive barrier, so that they touch. When two gold particles touch, they stick together, forming a rigid bond between spheres. This type of aggregation is called reaction-limited or chemically limited aggregation, since the aggregation rate depends upon the surface chemistry of the sphere.

By adding larger amounts of pyridine to the colloid, we can completely eliminate the charge on the spheres. Then there is no repulsive barrier between the spheres; they freely diffuse until they contact another sphere, at which point they stick together. The rate of the aggregation is limited only by how fast the Brownian particles diffuse into one another; hence this process is called diffusion-limited aggregation. After two particles stick together, the resulting cluster then continues to diffuse in the suspension. While clusters can grow from contacting more spheres, most growth occurs when clusters contact other clusters. Therefore this process is more fully referred to as diffusion-limited cluster-cluster aggregation, wile when the repulsive barrier remains we have reaction-limited cluster-cluster aggregation.

The two limiting cases of aggregation produce different types of clusters.[2] DLCA produces more ramified clusters, with a fractal dimension of ~ 1.8. RLCA produces denser clusters, with $d_f \sim 2.1$; this is because when two clusters come together under reaction-limited conditions, they can interpenetrate before they stick together, making the resultant cluster denser than it would be under diffusion-limited conditions. The growth rates are different for the two classes, with RLCA being much slower than DLCA, since each cluster must make many attempts before it can stick to another cluster. DLCA clusters show a power-law growth in time, while RLCA clusters grow exponentially. Finally, the distribution of cluster masses is different. These have been determined through analysis of transmission electron micrographs of aggregated samples.[28] DLCA produces a nearly flat distribution of cluster masses, up to some maximum mass, in agreement with the predictions based on the Smoluchowski equation description of the aggregation using a constant kernel. By contrast, RLCA produces clusters with a highly polydisperse distribution;[29] the number of clusters $N(M)$ with mass M scales as $M^{-\tau}$, with $\tau=1.5$, which compares well with theoretical predictions.[30]

The distribution of cluster masses plays an important role in light scattering. When $kR_g \gg 1$, the scattered intensity is proportional to the cluster mass. Thus clusters produced under diffusion-limited conditions, where $N(M)$ is constant to a cutoff mass, are relatively monodisperse for light scattering. By contrast, the power-law distribution of RLCA complicates the interpretation of QELS data because τ is sufficiently large that clusters of all sizes contribute appreciably to Γ_1. Since our interest here is to isolate the contribution of rotational diffusion, we restrict our attention to clusters formed by DLCA; examination of the combination of the effects of cluster mass distribution and rotational diffusion for RLCA clusters will be examined in a later work.[31]

Our experimental setup consists of an Ar-ion laser using the 4880-Å line at low power. We ensure that less than 1 mW is incident on the cell. This is essential to eliminate artifacts caused by sample heating due to the absorption of the colloid. The scattered light is imaged onto a photomultiplier tube mounted on an arm of a goniometer, with the sample fixed at the center. The detector arm is rotated between 10° and 150° from the forward direction, to vary the scattering wave vector. The intensity autocorrelation function is determined with an autocorrelator with 264 real-time channels. The entire setup is operated under computer control, facilitating both acquisition and analysis of the QELS data. This setup also allows the determination of the static structure factor of the aggregates.

The scattering volume in our experiments is $\sim 10^{-6}$ cm^3. To determine the importance of the various terms in the autocorrelation function, we calculate the density of clusters in our sample,

$$\rho=\frac{\rho_0\int_1^{M_c}N(M)dM}{\int_1^{M_c}MN(M)dM}, \quad (28)$$

where ρ_0 is the initial density of gold spheres before aggregation, $N(M)$ is the mass distribution function, which we approximate by assuming a sharp cutoff mass. The mass M is expressed in units of the mass of a gold sphere, so the lower limit of the integrals is 1. In our experiments, ρ_0 is generally 1.7×10^{12} cm^3. For diffusion-limited aggregation, $N(M)$ is a constant, and $\rho=2\rho_0/M_c$. Thus when the largest clusters are ~1 μm in radius, $M_c\approx7000$, making the number of clusters in the scattering volume around 500. Thus we do not have to worry about small number effects until the largest clusters reach a size greater than 5 μm. For reaction-limited clusters, due to the power-law distribution, there are always a large number of small clusters in the sample, compared to the diffusion-limited case. Since $\tau\approx1.5$, $\rho=\rho_0(1-M_c^{-1/2})/(M_c^{1/2}-1)$; if the cutoff radius is 2 μm, the number of clusters in the scattering volume will be ~5000, again making small-N effects unimportant.

We investigate the effects of rotational diffusion by examining the wave-vector dependence of the autocorrelation function obtained from a sample aggregated under diffusion-limited conditions. The size of the aggregates is carefully chosen so that $kR_g<1$ at the smallest angles and $kR_g>1$ at larger angles. This allows the true hydrodynamic radius to be measured at small angles, where the effects of rotational diffusion are negligible. From this value of the hydrodynamic radius, we can determine the cutoff mass M_c that characterizes the distribution of clusters in the sample. The effects of rotational diffusion can then be investigated by measuring the autocorrelation function at larger angles. The desired sample is obtained by allowing the colloid to aggregate to the appropriate point and then adding a small amount of surfactant to the solution. The surfactant bonds to the surface of the gold, providing steric stabilization and arresting any further aggregation. Separate measurements ascertain that the thin layer of surfactant does not affect either the static or dynamic light scattering from the aggregates.

We first investigate the effects of rotational diffusion on the shape of the autocorrelation function. An autocorrelation function, measured at 60°, for a sample where $kR_g>1$ and the effects of rotational diffusion are important, is shown in Fig. 8. From measurements at small k, where rotation is unimportant, we find $M_c=700$. The autocorrelation function, calculated without rotational diffusion for a cluster distribution flat up to M_c, is shown by the dotted curve in Fig. 8. As can be seen, the decay calculated without rotational diffusion is much slower than the measured decay. The increased decay rate is due to the rotational diffusion of the clusters; the solid line in Fig. 8 displays the autocorrelation function calculated using Eq. (9) with the same flat mass distribution of simulated DLCA clusters. The inclusion of rotational effects is crucial to explain the measured autocorrelation function for $kR_g>1$. We note that while the autocorrelation function in Fig. 8 is not a single exponential, its logarithm does not exhibit much curvature; this is due to the relatively dense distribution of decay rates, which tends to reduce the curvature of the logarithm of the sum of the decays.

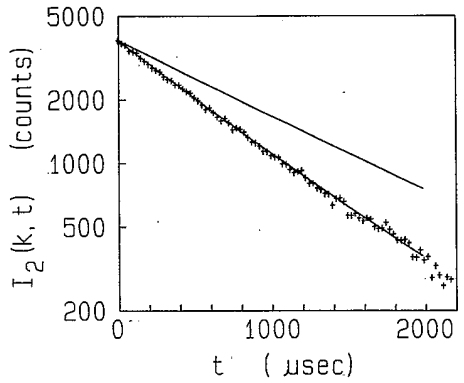

FIG. 8. Intensity autocorrelation function for a sample of aggregated colloid, measured at 60°. The data (crosses) are not normalized by the background value. The dashed line shows the calculated autocorrelation function ignoring rotational effects for a flat distribution of clusters, with the cutoff mass chosen to yield the decay rate measured at small scattering angles, where rotational effects are negligible. The solid line is the calculated autocorrelation function including rotational effects.

We can investigate the effects of rotational diffusion in more detail by examining the first cumulant Γ_1 of the measured decay as a function of scattering wave vector. Experimentally, we adjust the sample time of our correlator so that the autocorrelation function measured at each angle decays by about a factor of 20. The baseline is determined both from the total number of counts and from extra channels of the correlator delayed by an additional 1024 delay times. Both these measures agree to within $\sim0.1\%$. We subtract the baseline from the measured autocorrelation function, and take the logarithm of the result. We then perform a fourth-order polynomial fit on this data, with the first cumulant coming from the linear term of the fit. Ideally the cumulant should be calculated in the limit of $t\rightarrow0$; in practice, reducing the amount of data fitted to approach the zero time limit does not appreciably change the measured cumulant for our data. Thus we are confident that we are obtaining a valid experimental measure of the first cumulant.

In Fig. 9 we show experimental measurements of Γ_1/k^2 as a function of k. The k-independent behavior of Γ_1/k^2 at small k, indicative of purely translational motion, is evident. The k dependence seen at higher k would not be observed for a monodisperse system of isotropic scatterers. The polydispersity of DLCA can introduce only a small-k dependence to Γ_1/k^2; any further dependence is due to rotational effects. As can be seen in Fig. 9, at large wave vectors, the measured value of Γ_1/k^2 is a factor of 2 higher than the small wavelength limit. This demonstrates that the contribution of rotational diffusion to Γ_1 is almost as large as the translational contribution. Thus the effects of rotational diffusion must be included in the determination of the true hydro-

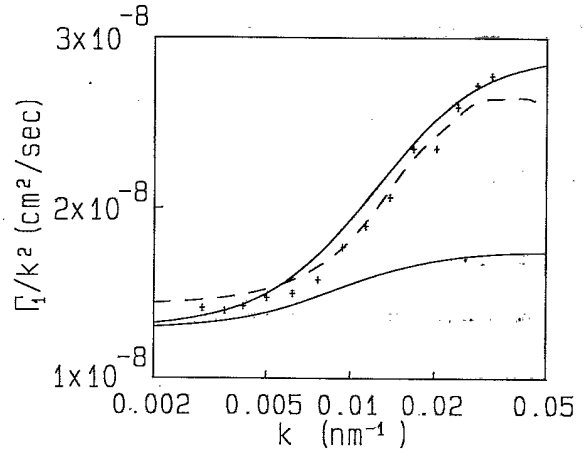

FIG. 9. Γ_1/k^2 vs k for an ensemble of DLCA clusters. The crosses are experimental data, the dashed lines are cumulants calculated from the multipole expansion terms using a flat cluster mass distribution with $M_c=500$. The upper solid line shows the cumulants calculated from the scaling of multipole expansion terms using a self-preserving mass distribution with $\overline{m}=220$ particles. The lower solid line shows calculated results with the self-preserving distribution not including rotational effects.

dynamic radii of the clusters from the measured cumulant when $kR_g \gtrsim 1$.

The dashed line in Fig. 9 shows Γ_1/k^2 calculated using Eq. (27) for a distribution of clusters produced by computer simulation of DLCA. Thus, we use 20 computer-simulated clusters each for masses of 100, 200, 300, 400, and 500. The flat cluster mass distribution corresponds to that expected for DLCA, while the upper cutoff mass is chosen to obtain the best fit to the data at small k. The clusters have $d_f=1.8$, in agreement with that measured experimentally, while we chose $\beta=0.87$ as computed for DLCA clusters.[23,24] The agreement between the calculation and the data is very good. The major deviation appears at large k, where the data are somewhat higher than predicted by our calculation. This is presumably due to our choice of cluster mass distribution, which has a sharp cutoff. A more realistic cluster mass distribution would have an exponential cutoff which decays more slowly than the one used here.

Rather than generate computer-simulated clusters to exactly replicate the expected cluster mass distribution of DLCA, we have adopted an alternative approach which takes advantage of the scaling of the first cumulant, shown for DLCA clusters in Fig. 7. Thus we replace the first cumulant by the effective value given in Fig. 7 and weight it by the radially averaged structure factor. In doing so we have

$$\Gamma_1(k)=\frac{\sum_M \Gamma_1(kR_M)S(kR_M)M^2N(M)}{\sum_M S(kR_M)M^2N(M)}, \quad (29)$$

where $S(kR)$ is the scaled static structure factor for DLCA clusters and $N(M)$ is the cluster mass distribution.

It is instructive to examine the physics implicit in Eq. (29). The scattering intensity for each cluster is $I(M)=M^2S(kR_M)$. For $kR_M \ll 1$, the phase of the scattered electric field from each particle is identical at the detector and adds coherently, so the scattered intensity is proportional to M^2. Since for these small clusters $S(kR_M)=1$, we have $I(M)=M^2$, as expected in Eq. (29). If the cluster is larger than k^{-1}, the scattered phases no longer add coherently. We can treat the cluster as being made up of subunits of volume k^{-3}, with each subunit scattering coherently, while the fields from different subunits add randomly, The subunits have mass $m_0(ka)^{-d_f}$, where m_0 and a are the mass and radius of the constituent particles. The scattered intensity from each subunit is proportional to the square of its mass, $m_0^2(ka)^{-2d_f}$. The number of subunits in a cluster is $M/m_0(ka)^{-d_f}$. Thus, for $kR_M \gg 1$, the random addition of the phases of the scattered fields from each subunit results in

$$I(M)=[m_0(ka)^{-d_f}]^2\frac{M(ka)^{d_f}}{m_0}$$
$$=M^2(kR_M)^{-d_f}=M(ka)^{-d_f}. \quad (30)$$

Since for these large clusters $S(kR_M)\approx(kR_M)^{-d_f}$, in Eq. (29), we lose one power of M and have $I(M)=M(ka)^{-d_f}$ as expected. However, the fluctuations of the phase factor which cause the decrease in the scattering intensity from the simple M^2 dependence yield this result only in the ensemble average over all orientations; for any given orientation, the phases form the subunits add to give fluctuations about this average. The contributions of these fluctuations due to rotational diffusion of the cluster are the subject of this paper. Within the approximation of Eq. (29), this additional contribution is contained in the effective diffusion coefficient Γ_{eff}.

Calculation of Γ_1/k^2 for the flat distribution used before gives results that are virtually identical to those shown in Fig. 9 using the more exact calculation with Eq. (27). This confirms the appropriateness of our approximation and provides a relatively simple method for extending our previous treatment to include the effects of rotation for more general forms of the cluster mass distribution, and for larger clusters than is possible with direct calculations. For diffusion-limited cluster aggregation, we represent the cluster mass distribution by the self-preserving distribution derived from a constant kernel solution to the Smoluchowski equations[32]

$$N(m_i)=\frac{N_T}{\overline{m}}\left[1-\frac{1}{\overline{m}}\right]^{i-1}, \quad (31)$$

where m_i is the mass of a cluster made of i particles, $\overline{m}$ is the mean cluster mass, and N_T is the total number of clusters of all masses. The value of $\overline{m}$ is set by the experimentally measured values of Γ_1/k^2 at small wave vectors. After $\overline{m}$ is defined, there are no adjustable parameters in the calculation of Γ_1 from Eq. (29). The results from these multipole expansion calculations are shown by the solid line in Fig. 9. The agreement is excellent. The

calculated cumulants match both the magnitude of the wave-vector dependence of the experimental data and the range of k space over which the dependency occurs, clearly indicating the usefulness of our multipole expansion approach. The lower curve in Fig. 9 shows how Γ_1/k^2 varies if only cluster mass distribution effects are included, demonstrating that most of the wave-vector dependence is due to rotational diffusion of the clusters.

Finally, we note that even though the k dependence of Γ_1/k^2 due to rotational diffusion is quite pronounced when plotted in Fig. 9, the dominant k dependence of the first cumulant is the k^2 dependence of the translational motion. Thus a plot of Γ_1 as a function of k^2 will not discern this additional k dependence due to the rotational effects. Nevertheless, when plotted in the more sensitive fashion of Fig. 9, the effects are clear.

CONCLUSION

In this paper we have investigated the effects of rotational diffusion of fractal aggregates on quasielastic light scattering. When $kR_g > 1$, we have shown that these effects are substantial. They are determined by a multipole expansion of the scattering from the aggregates, using computer-simulated clusters. They show that the clusters are anisotropic at all length scales, and that this anisotropy is independent of cluster mass. We also examined the consequences of the contribution of purely rotational terms to the homodyne autocorrelation function, and the applicability of the Siegert approximation relating homodyne and heterodyne autocorrelation functions. For typical experimental conditions, the use of the Siegert approximation was shown to be valid, with pure rotational terms making a negligible contribution. We demonstrated the important effect of the rotational diffusion on the experimentally measured autocorrelation functions by examining the wave-vector dependence of the first cumulant measured for gold clusters aggregated under diffusion-limited conditions. The calculated multipole terms were used to determine the first cumulant of the autocorrelation function from an ensemble of clusters matching the cluster mass distribution produced under the experimental conditions. Excellent agreement was obtained between the calculations and the experimental measurements. The effects of rotational diffusion were found to change the measured first cumulant by a factor of nearly 2, demonstrating the importance of including these effects in interpreting QELS data from fractal colloid aggregates. Finally, we also presented a determination of the scaling of the effective diffusion coefficient obtained from the first cumulant. At small kR_g this reflects translational diffusion only, while at large kR_g it includes the effects of rotational diffusion. The scaling of the effective diffusion coefficient can be used to correct measured data for the effects of rotational diffusion, and thus to obtain a true hydrodynamic radius, even when $kR_g > 1$.

ACKNOWLEDGMENT

One of us (R.K.) acknowledges the financial support and hospitality of Exxon Research and Engineering Company.

[1] *Kinetics of Aggregation and Gelation,* edited by F. Family and D. P. Landau (North-Holland, Amsterdam, 1984).
[2] D. A. Weitz, M. Y. Lin, and J. S. Huang, in *Physics of Complex and Supermolecular Fluids,* edited by S. A. Safran and N. A. Clark (Wiley-Interscience, New York, 1987), p. 509.
[3] D. A. Weitz, M. Y. Lin, J. S. Huang, T. A. Witten, S. K. Sinha, and J. S. Gethner, in *Scaling Phenomena in Disordered Systems,* edited by R. Pynn and A. Skjeltorp (Plenum, New York, 1985), p. 171.
[4] P. Meakin, Phys. Rev. Lett. **51**, 1119 (1983).
[5] M. Kolb, R. Botet, and R. Julien, Phys. Rev. Lett. **51**, 1123 (1983).
[6] H. M. Lindsay, M. Y. Lin, D. A. Weitz, P. Sheng, Z. Chen, R. Klein, and P. Meakin, Faraday Discuss. Chem. Soc. **83**, 153 (1987).
[7] P. N. Pusey, in *Photon Correlation Spectroscopy and Velocimetry,* edited by H. Z. Cummins and E. R. Pike (Plenum, New York, 1976), p. 45.
[8] T. C. Halsey, P. Meakin, and I. Procaccia, Phys. Rev. Lett. **56**, 854 (1986).
[9] D. A. Weitz and M. Oliveria, Phys. Rev. Lett. **52**, 1433 (1984).
[10] P. Dimon, S. K. Sinha, D. A. Weitz, C. R. Safinya, G. S. Smith, W. A. Varady, and H. M. Lindsay, Phys. Rev. Lett. **57**, 595 (1986).
[11] D. A. Weitz, J. S. Huang, M. Y. Lin, and J. Sung, Phys. Rev. Lett. **54**, 1416 (1985).
[12] R. Pecora, J. Chem. Phys. **40**, 1604 (1964).
[13] R. Pecora, J. Chem. Phys. **48**, 4126 (1968).
[14] B. Chu, *Laser Light Scattering* (Academic, New York, 1974).
[15] B. J. Ackseron, T. W. Taylor, and N. A. Clark, Phys. Rev. A **31**, 3183 (1985).
[16] B. J. Berne and R. Pecora, *Dynamic Light Scattering* (Wiley-Interscience, New York, 1976).
[17] Z. Chen, P. Sheng, D. A. Weitz, H. M. Lindsay, M. Y. Lin, and P. Meakin, Phys. Rev. B **37**, 5232 (1988).
[18] D. W. Schaeffer and B. J. Berne, Phys. Rev. Lett. **28**, 475 (1972).
[19] H. M. Lindsay, R. Klein, D. A. Weitz, and P. Meakin (unpublished).
[20] G. Seeley, T. Keyes, and T. Ohtsuki, Phys. Rev. Lett. **60**, 290 (1988).
[21] P. Meakin and F. Family, Phys. Rev. A **34**, 2558 (1986).
[22] P. Meakin, F. Leyvraz, and H. E. Stanley, Phys. Rev. B **31**, 564 (1985).
[23] W. Hess, H. L. Frisch, and R. Klein, Z. Phys. B **64**, 65 (1986); equation (4) in this paper must be corrected: the 4 should be replaced by 2.
[24] Z.-Y. Chen, P. Meakin, and J. M. Deutch, Phys. Rev. Lett. **59**, 2121 (1987).
[25] P. Wiltzius, Phys. Rev. Lett. **58**, 710 (1987).
[26] R. Ball (private communication).
[27] D. A. Weitz, M. Y. Lin, and C. J. Sandroff, Surf. Sci. **158**, 147

(1985).
[28]D. A. Weitz and M. Y. Lin, Phys. Rev. Lett. **57**, 2037 (1986).
[29]J. E. Martin and F. Leyvrax, Phys. Rev. A **34**, 2346 (1986).
[30]R. C. Ball, D. A. Weitz, T. A. Witten, and F. Leyvraz, Phys. Rev. Lett. **58**, 274 (1987).
[31]M. Y. Lin, H. M. Lindsay, D. A. Weitz, and R. Klein (unpublished).
[32]P. G. J. Von Dongen and M. H. Ernst, Phys. Rev. Lett. **54**, 1396 (1985).